Highly Efficient MPP Tracker Based on Adaptive Neuro-fuzzy Inference System for Stand-Alone Photovoltaic Generator System

Mohamed H. Osman*‡, Mohamed A. El Seify*, Mamdouh K. Ahmed**, Nikolay V. Korovkin***, Ahmed Refaat****

*Electrical Engineering Department, Al-Azhar University, Qena, 83513, Egypt

** Electrical Engineering Department, Al-Azhar University, Cairo, 11751, Egypt

*** Institute of Energy, Peter the Great Saint-Petersburg Polytechnic University, Saint-Petersburg, 195251, Russia

**** Electrical Engineering Department, Port Said University, Port Said, 42524, Egypt

(mo_hassan87@yahoo.com, mohamed_1988@azhar.edu.eg, Engmamdouhkamal@yahoo.com, nikolay.korovkin@gmail.com, ahmed_refaat_1984@eng.psu.edu.eg)

‡Corresponding Author; Mohamed H. Osman, 83513, Tel: +201033535996, mo_hassan87@yahoo.com

Received: 06.12.2021 Accepted: 13.01.2022

Abstract- Maximum Power Point Tracking (MPPT) methods are being developed to increase the power delivered by the photovoltaic (PV) systems. Recently, AI-based MPPT controllers have been extensively utilized for PV generator systems. Among these various AI methods, the Adaptive Neural Fuzzy Inference System (ANFIS) is widely used to capture the maximum power from the PV systems. Obtaining precise data for training and tuning the ANFIS model, on the other hand, presents a considerable challenge in establishing an effective ANFIS-MPPT technique. This article proposes a highly efficient MPP tracker based on adaptive ANFIS with direct control for stand-alone PV generators, which trace the MPP under rapidly changing solar radiation and cell temperatures. In this technique, the training data are extracted with the aid of a multi-variable step perturbation and observation (MV-P&O-MPPT) algorithm to avoid the errors that are usually included in an experimental dataset. Further, the boost converter's duty cycle is directly adjusted, eliminating the PI control loop. The proposed ANFIS-MPPT technique is simulated and compared with the Artificial Neural Networks (ANN), and Fuzzy Logic Controller (FLC) reported in the literature. Considering the outcomes of these approaches, the ANFIS-MPPT controller precisely traces the MPP and achieves higher efficiency under different climatic conditions.

Keywords Adaptive Neuro-Fuzzy Inference System, MPPT, Photovoltaic, Fuzzy Logic Control, Artificial Neural Networks.

1. Introduction

The output power of the photovoltaic system is affected by environmental conditions, for instance, temperature and solar radiation. The MPPT techniques increase the PV power generating efficiency [1],[2]. In general, several issues (i.e., application type, sensors used, efficiency, and cost) should be considered when aiming to propose a PV MPPT controller [3],[4]. Traditional and artificial intelligence (AI) approaches are the two basic categories of these techniques[5,6]. Both Incremental Conductance (IC) [7] and Perturbation and Observation (P&O) [8] are the most extensively utilized traditional methods. On the other hand, the fuzzy logic controller (FLC) [1], [9], the artificial neural network (ANN) [10], and the adaptive neuro-fuzzy inference system (ANFIS) [11] are well-known AI techniques.

The P&O method is commonly employed for PV-MPPT because of its simplicity and relatively inexpensive; though, it suffers from different issues like low tracking speed, excessive oscillation, and drift problems correlated with the fast-changing radiation [12],[13]. Hence, the IC-MPPT is established to fix the shortcomings of the P&O method. The ability to attain the Maximum Power Point (MPP) under rapidly changing environmental circumstances [14], [15] is

the key benefit of this technique. However, imbalanced and measurement error is an enormous problem that faces the operation of a PV system because it uses a derivative operation [16]. Therefore, several modifications have been introduced for defeating the challenges of IC-MPPTs and P&O [12], [15], and [17], but they are counted as deficient solutions. In contrast, AI techniques have been suggested to overcome these difficulties, where it does not require accurate parameters or complex mathematics for systems design. These methods mainly depend on the FLC [1], [9], and the ANN [18]. Furthermore, they provide more precise and flexible control, particularly in non-linear systems.

The FLC is rated as a highly efficient controller of a PV system because of its higher tracking speed and lower oscillation contrasted to classical MPPT methods [19]. Notwithstanding, the challenge of selecting appropriate membership functions is still unsolved. Further, it requires extensive calculations and considerable data storage [20], [21]. The ANN is regarded as another effective technique for non-linear systems like PV modules. It generates the heuristic output by means of the quantification of the real numerical data. Nonetheless, black-box operation and slow training are the major drawbacks of the ANN system [22].

An ANFIS is a combination of ANN and FLC employed to overcome the limitations of the previous approaches. ANFIS is one of the most robust AI strategies since it combines the benefits of ANN and FLC [11]. Combining ANN with FLC appears to be more appealing in terms of combining ANN's learning skills with FLC's ability to handle erroneous information, which seems more appropriate for PV applications [23]. MPP tracking using various ANFIS controller topologies is described in the literature. However, all methodologies are analogous, and it depends on the type of the parameters input, estimation of the output parameters, the electrical converter employed, and the number of membership functions (MFs).

However, to create the ANFIS-MPPT controller, the main challenge is collecting enormous training data. Experimental data for ANFIS-MPPT training were applied in [24,25]. Nonetheless, there are significant issues with the experimental data, such as its narrow dynamic range. Furthermore, practical data collection frequently includes mistakes, and the acquired data is only applicable to a given geographical place. On the other hand, in [26], the training dataset was achieved by stimulating the PV module. The proposed technique involved two stages in determining the duty cycle, which made it more complicated. In [27], the authors employ the open-circuit voltage and short-circuit current input to the ANFIS-MPPT controller. Nevertheless, it does not trace the exact MPP due to the approximation used. Irradiation and temperature were employed in [28, 29] to train the ANFIS-MPPT controller. Nonetheless, the insufficient training data set results in a rather large training error.

In this article, a novel direct control method based on the ANFIS model has been utilized. In this technique, the duty cycle can be adjusted immediately in the MPPT method, and the computational and evaluation process for tuning the gains of the PI controller is no longer required. Further, the training data for the suggested technique are extracted with the aid of a multi-variable step perturbation and observation (MV-P&O-MPPT) algorithm for avoiding the errors usually included in an experimental dataset. The proposed ANFIS-based MPPT controller's competence has been verified compared to ANN-MPPTs and FLC-MPPTs. The simulation result demonstrated that the suggested ANFIS-MPPT controller has the best tracking speed, highest power, least MPP oscillation, and is robust with sudden changes in weather conditions.

2. ANFIS Technique

ANFIS has the neural network's learning capabilities which can improve the performance of intelligent systems using just a priori information. It mainly depends on the hypothesis of the Takagi–Sugeno-type FIS. ANFIS builds a Fuzzy system and adjusts the membership function's parameters by using a specific input-output dataset. ANFIS, like neural networks, has a network-type structure and uses fuzzy membership functions to map the input-output dataset. Fig.1 illustrates the Takagi-Sugeno two-rule system-based ANFIS design with a single output (Y) and multiple inputs (M and N). Here, fuzzy membership functions for the inputs M and N are a_1, a_2, and b_1, b_2, respectively. A Takagi-Sugeno ANFIS contains the following two rules:

if M is a_1 and N is b_1 , then $f_1 = r_1 M + s_1 N + t_1$ (1)

if M is a_2 and N is b_2 , then $f_2 = r_2 M + s_2 N + t_2$ (2)

where r_j , s_j , and t_j are the consequence parameters.

In general, the ANFIS design includes five layers, as indicated in figure1. These layers are described in detail as follows:

Layer 1

In layer 1, the number of nodes is based on the input membership function's number. Each one is an adaptive node, and their output is represented by:

$$O_{1,j} = \mu a_j(M) \text{ for } j = 1,2 \quad (3)$$

$$O_{1,j} = \mu b_{j-2}(N) \text{ for } j = 3,4 \quad (4)$$

where μ , and $O_{1,j}$ exhibit the membership function and its value for the inputs M and N, respectively.

The number of layers and nodes in the training data are denoted respectively by the subscripted 1, and j . The membership function "μ" can take the form of Gaussian, trapezoidal, or triangular shapes. The generalized bell is usually employed to describe the shape of the membership function. It is expressed by the following equation:

$$\mu a(M) = \frac{1}{1 + \left| \frac{M - u_j}{v_j} \right|^{2w_j}} \quad (5)$$

where w_j, u_j, and v_j are the membership function coefficients, also known as premise coefficients, and should be optimized throughout the training phase.

Layer 2

This layer's nodes are all fixed nodes, take the output (the value of memberships) from the previous layer, and their output is given by equation (6).

$$O_{2,j} = z_j = \mu a_j(M)\mu b_j(N) \quad \text{for} \quad j = 1,2 \tag{6}$$

Layer 3

In layer 3, each node is considered as a fixed layer node, which is utilized to scale the firing strength, as illustrated in equation (7).

$$O_{3,j} = \bar{z}_j = \frac{z_j}{z_j + z_j} \tag{7}$$

Layer 4

In this layer, the rule consequent utilized to calculate and adapt each node using the following relation:

$$O_{4,j} = \bar{z}_j f_j = \bar{z}_j (r_j M + s_j N + t_j) \tag{8}$$

Layer 5

Finally, to obtain the final output, all input signals in this layer will be added together, as given by the following expression:

$$O_{5,j} = \sum_j \bar{z}_j f_j = \frac{\sum_j z_j f_j}{\sum_j z_j} \tag{9}$$

where z_j is the minimum number of membership functions and f is the output membership function center value.

The ANFIS model's training operation is based on the number of iterations. Layer 4 determines the output nodes in every iteration, whereas layer 5 determines the subsequent parameters. The ANFIS model is trained using a hybrid technique, which combines back-propagation (BP) with least square estimation (LSE) to optimize the premise and its associated coefficients [30].

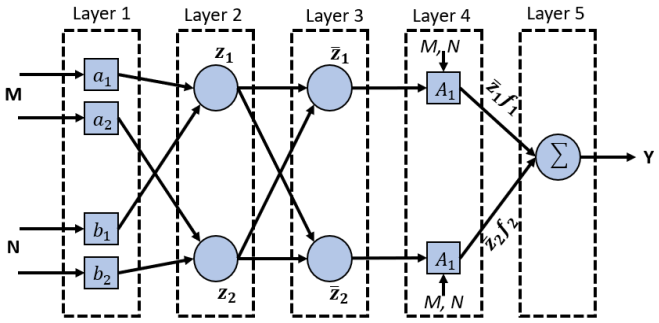

Fig. 1. ANFIS structure.

3. Propose ANFIS-MPPT Algorithm

In this paper, direct tuning of the duty cycle is performed in the ANFIS-MPPT approach and eliminated the PI control loop. In this way, the control loop of the MPPT is simplified and avoids the estimation process for adjusting the gain of the PI controller. In the proposed ANFIS-MPPT technique, the PV panel's radiation (G) and temperature (T) are the input parameters. Whereas the output parameter is the optimum duty cycle (D_m), as displayed in Fig. 2. Fig. 3 illustrates the typical duty cycle (D_m) at MPP with radiation (G) change under three different operational ambient temperatures (T). It depicts that the relationship of D_m with the weather factors (G and T) is not complicated.

Furthermore, the relationship between the output parameter (D_m) and the input parameters (G and T) appears to be a flat unimodal arch. Thus, following a thorough training period, the ANFIS approach can accurately forecast the D_m value as a function of climatic conditions. The first step in building the MPPT-ANFIS controller is to acquire an input-output dataset for training purposes. The training data is created with the help of the MV-P&O-MPPT algorithm proposed in [31]. The flowchart in Fig. 4 shows steps of the method for creating the dataset.

Step 1: Simulate the PV system with a single diode model and multi-variable P&O MPPT algorithm.

Step 2: Apply the obtained G and T in the suggested PV system.

Step 3: Examine the PV output power until it captures MPP, then record the corresponding duty cycle D_m.

Step 4: These generated data will be employed for training and testing the ANFIS model, and it will be organized in an array format with two columns for inputs (T and G) and one column for outputs (D_m) data.

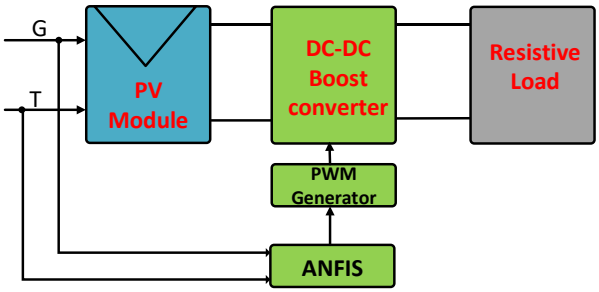

Fig. 2. PV system block diagram with ANFIS-MPPT.

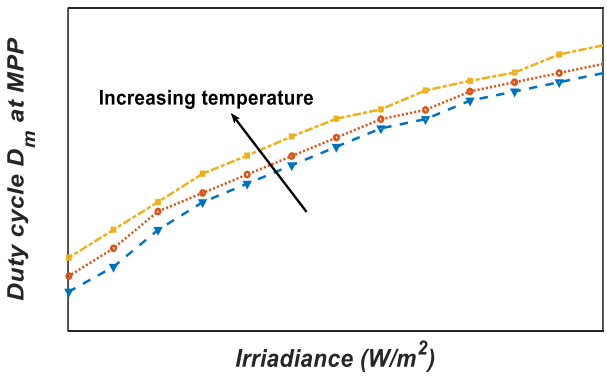

Fig. 3. Duty cycle (D_m) versus irradiance at varying temperatures.

4. Tuning of ANFIS model

The first stage in designing the MPPT controller utilizing the ANFIS technique is to collect the training data set. These data are obtained employing an efficient PV model with the MV-PO MPPT algorithm. With large-scale variations in operating temperature and solar irradiation, acquiring training data is crucial. As a result, the radiation spectrum is partitioned into several periods (17 periods) ranging from 200 W/m^2 to 1000 W/m^2 with a step size of 50 W/m^2. In contrast, the cell temperature span is partitioned into 9 periods ranging from 10 °C to 50 °C with a stride size of 5 °C. The duty cycle regarding the MPP (D_m) is recorded for each pair of input data. Ultimately, this creates 153 training datasets. A sample of the training data set is depicted in Table 1.

To create the FIS, the number of MFs for T and G is set to seven and nine, sequentially, since the influence of irradiance on PV curves is greater than that of cell temperature. This produces 63 fuzzy rules, as illustrated in Fig. 5. MATLAB's ANFIS editor provides several types for the input and the output MFs. Table 2 outlines the Mean Square Error (MSE) of various MFs over 100 epochs with a 0.1% percent error tolerance to find the best ones. As demonstrated in Fig. 6, the linear type for output MFs and the trimf type for input MFs are the best, with an MSE of 0.17 percent. Then, the hybrid optimization approach based on least-squares and back-propagation is utilized to develop and train the basic FIS model. The calculated (offline by simulation) and predicted (by applying the proposed model) D_m values are compared under the same atmospheric conditions, as demonstrated in Fig. 7. It shows that the output of ANFIS matches that calculated training data with a mean test error of 0.17%. Fig. 8 shows the 3D diagram between T, G, and D_m where D_m increases with ambient temperature and radiation intensity, as explained in Fig. 3.

Table 1. A sample of training data.

T	15 ºC	20 ºC	25 ºC	30 ºC
G	D_m	D_m	D_m	D_m
500	0.4106	0.421	0.421	0.4305
550	0.4413	0.4405	0.4511	0.4512
600	0.4612	0.4702	0.4702	0.4705
:	:	:	:	:
900	0.5622	0.5603	0.571	0.5715
950	0.5718	0.5804	0.5818	0.5818
1000	0.5808	0.5905	0.5922	0.5914

Table 2. The Mean Square Error for different types of MFs for the outputs and inputs of the ANFIS model.

Input MFs	Linear MFs Output		Constant MFs Output	
	MSE	No. of iterations	MSE	No. of iterations
gbellmf	0.002213	100	0.008462	100
psigmf	0.001822	10	0.006386	16
trimf	0.001708	25	0.007950	100
gauss2mf	0.002514	100	0.012000	100
dsigmf	0.001819	10	0.006283	16
trapmf	0.002558	100	0.012400	100
gaussmf	0.002720	100	0.008178	100
pimf	0.002498	100	0.013200	100

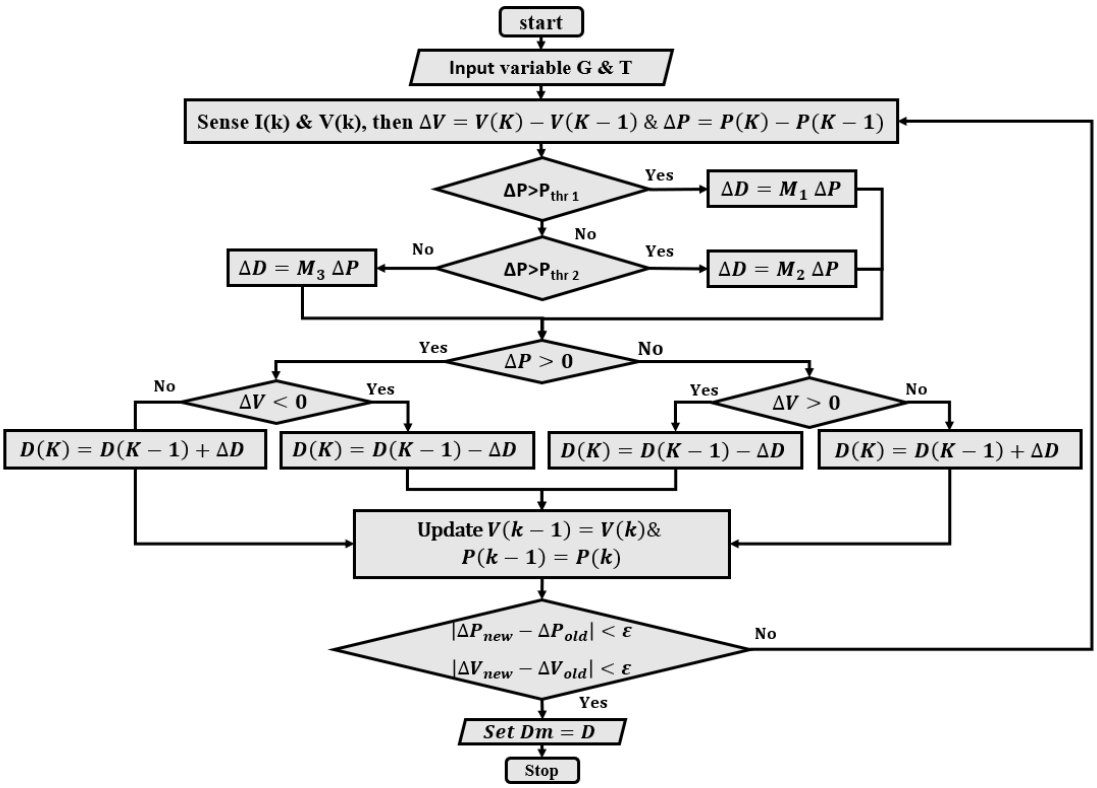

Fig. 4. Flowchart of the training data generation based on the MV-PO algorithm.

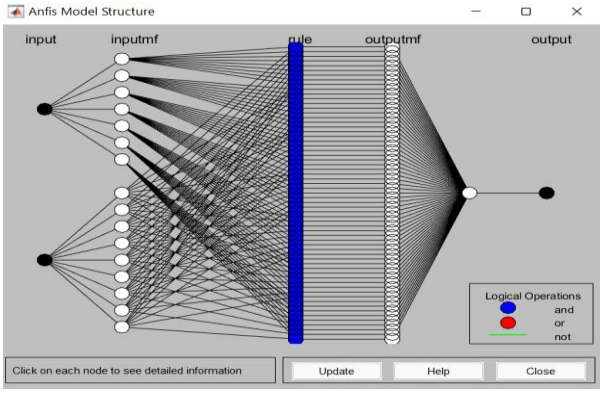

Fig. 5. The generated structure of the ANFIS model.

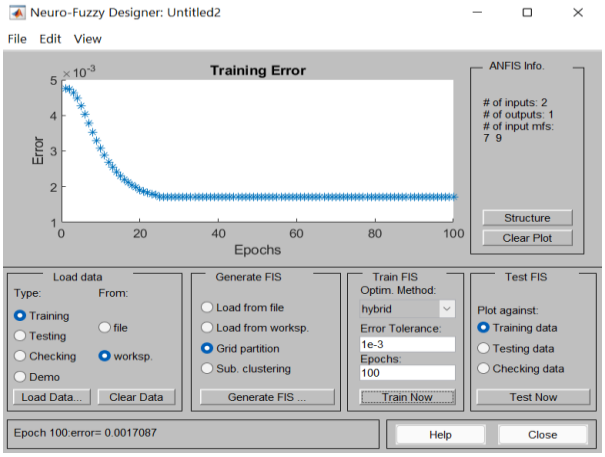

Fig. 6. ANFIS training error versus Epochs.

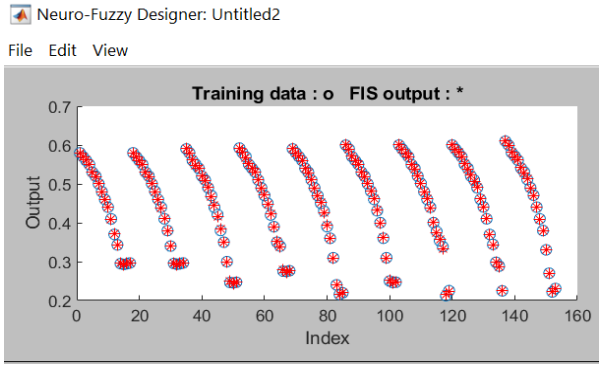

Fig. 7. ANFIS output versus training data.

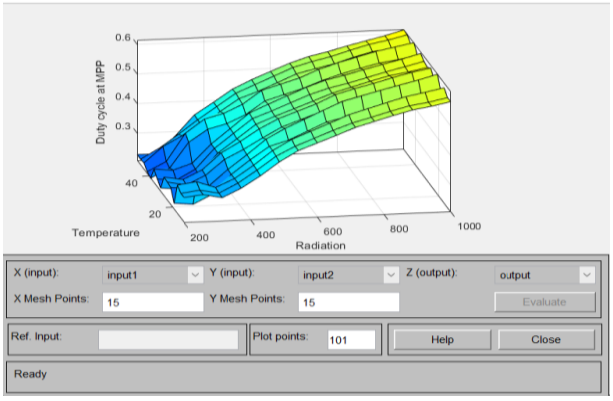

Fig. 8. G and T vs. D_m on a 3D surface.

5. Simulation and Results

The proposed controller (presented in Fig. 2) is numerically simulated using MATLAB/Simulink to test its performance. An industrial PV module (i.e., MSX-60) is selected for the simulation to fulfill the load's electrical demand, and its specifications are given in Table 3. As mentioned in [32], the PV module is modeled by a single diode. A DC-DC boost converter is employed as power conditioning equipment between the PV module and the load, and its components are specified in Table 4. As illustrated in Fig. 9, the temperature is assumed to be constant at 25 °C, and the solar irradiation is altered in decrements between the values 1000 W/m^2, 800 W/m^2, 600 W/m^2, 500 W/m^2, and 400 W/m^2. A comparison study between the performance of the ANFIS, ANN, and FLC techniques is represented in Fig. 10.

As displayed in the zoomed part of Fig. 11, the proposed ANFIS algorithm captures the MPP after 0.009 s (i.e., 1000 W/m^2 of radiation with a cell temperature of 25 °C) against 0.02 s the ANN method and 0.03 s for the FLC algorithm. For instance, the output power oscillates around the MPP with 0.02 % percent utilizing the proposed controller, compared to 0.05 % percent for the FLC and 1.07 % percent for the ANN algorithm at 600 W/m^2 of radiation intensity and cell temperature 25 °C (Fig. 12). Moreover, the efficiency of ANFIS-MPPT is demonstrated by comparing the error in maximum power for the three algorithms used, as illustrated in Fig. 13. It depicts that the ANFIS controller records the maximum power with low error at various operating conditions.

Table 3. Datasheet value of the MSX-60 Panel

PV Parameter	Symbol	Value
Voltage at MPP	V_{mpp}	17.04V
Current at MPP	I_{mpp}	3.55A
Power at MPP	P_{mpp}	60.53 W
Open Circuit Voltage	V_{oc}	21.1V
Short Circuit Current	I_{sc}	3.8 A

Table 4. DC-DC boost converter parameter

Parameter	Symbol	Value
Input voltage	V_{in}	17 V
Output voltage	V_{out}	40 V
Inductance	L	4 mH
Capacitor	C	100 µF
Switching frequency	F_s	10 kHZ

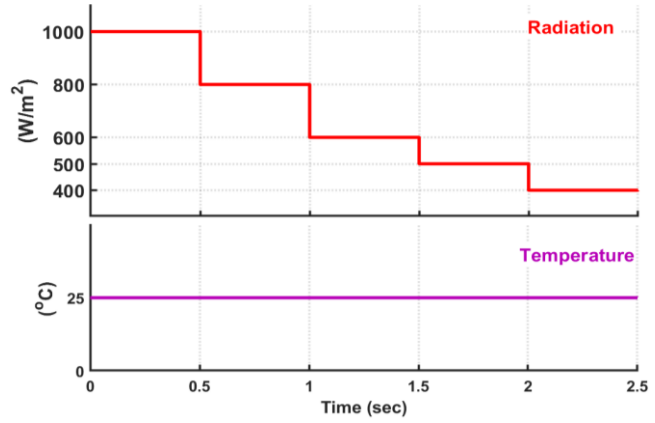

Fig. 9. Solar irradiation and temperature profile.

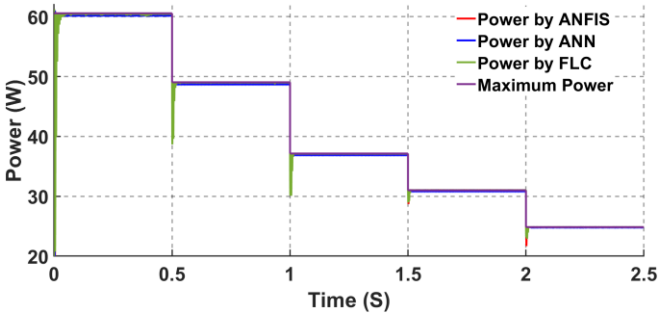

Fig. 10. Case1: Performance of the ANFIS vs. ANN and FLC MPPT algorithms.

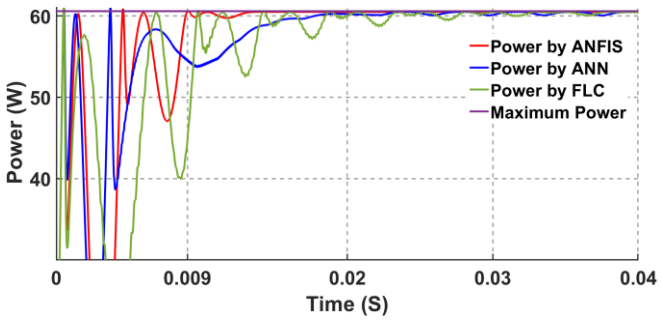

Fig. 11. Case1: Dynamic response of ANFIS vs. ANN and FLC MPPT algorithms.

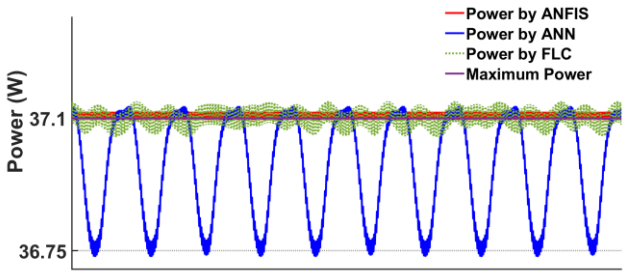

Fig. 12. Case1: Steady-state power oscillation produced by ANFIS vs. ANN and FLC MPPT algorithms.

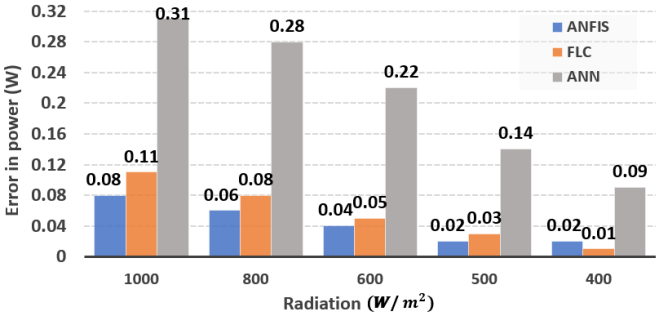

Fig. 13. Case1: Error in Pmax at different radiation levels and constant temperatures using ANFIS, FLC, and ANN techniques.

In the second case: as illustrated in Fig. 14, the temperature levels are varied at different values 50 °C, 40 °C, 30 °C, 20 °C, and 10 °C. On the other hand, solar radiation changes between 1000 W/m^2 and 400 W/m^2 with a decrement of 200 W/m^2. Fig. 16 depicts the power tracking convergence time of the three algorithms used (FLC, ANN, and ANFIS technique). The ANFIS controller is the fastest one with a tracking time of 0.009 s against 0.025 s for both ANN and FLC at the first level of irradiation. Additionally, the MPP oscillation is decreased to 0.05 % using the proposed controller (shown in Fig. 17) at an irradiation intensity of 600 W/m^2 and a temperature of 30 °C, compared to 0.13 % for the FLC and 0.46 % for the ANN algorithm. Further, Fig. 18 depicts the deviation in maximum power at different radiation levels and temperatures using the ANFIS, FLC, and ANN techniques. The ANFIS controller records the lowest percentage error in tracking the maximum power under all operational scenarios.

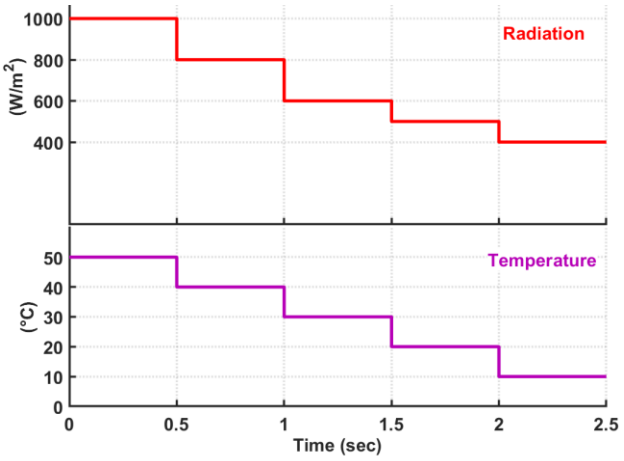

Fig. 14. Solar irradiation and temperature profile.

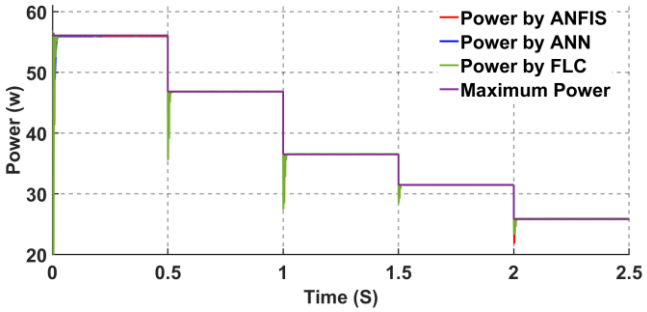

Fig. 15. Case 2: Performance of the ANFIS vs. ANN and FLC MPPT algorithms.

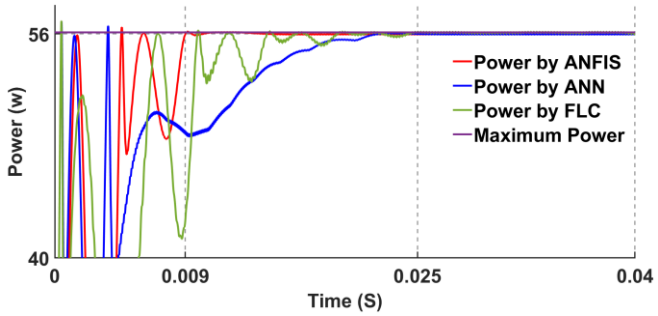

Fig. 16. Case 2: Dynamic response of ANFIS vs. ANN and FLC MPPT algorithms.

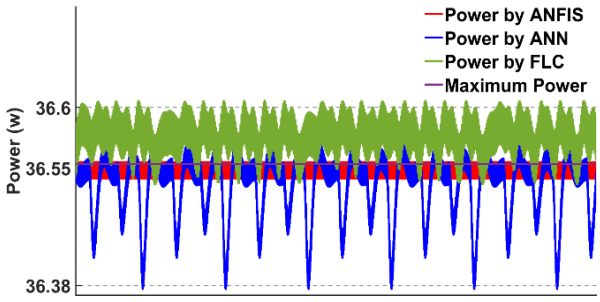

Fig. 17. Case 2: Steady-state power oscillation produced by ANFIS vs. ANN and FLC MPPT algorithms.

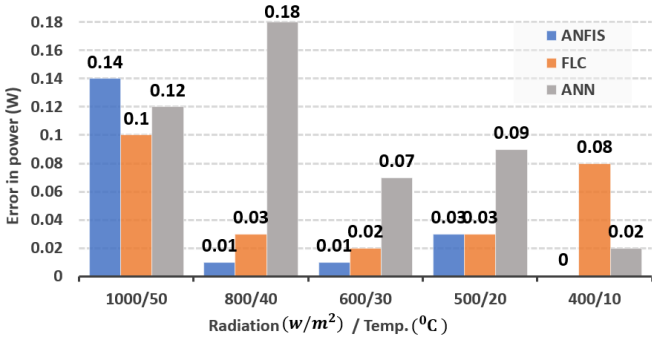

Fig. 18. Case2: Error in Pmax at different radiation levels and temperatures using ANFIS, FLC, and ANN techniques.

Similarly, this case (case 3) simulated the performance of ANFIS, ANN, and FLC techniques at a constant temperature (25 °C) with the variable solar illuminations (400 W/m^2, 500 W/m^2, 600 W/m^2, 800 W/m^2, and 1000 W/m^2 respectively), as displayed in Fig. 19. It can be seen from Fig. 20 and Fig. 21 that all methods capture the MPP simultaneously. Specifically, the tracking time is 0.015 s at (400 W/m^2 and 25 °C). A portion of the response (Fig. 22) is zoomed with irradiation level of 600 W/m^2 and cell temperature of 30 °C to illustrate the efficiency of the proposed ANFIS model in steady-state. It is observed from the zoomed part that the proposed ANFIS has a small smooth oscillation around the MPP as compared to ANN and FLC techniques. The error in extracted maximum power using the ANFIS, FLC, and ANN techniques at different radiation levels and invariant temperature (25 °C) is illustrated in Fig. 23. Under all operational conditions, the ANFIS controller properly records the maximum power.

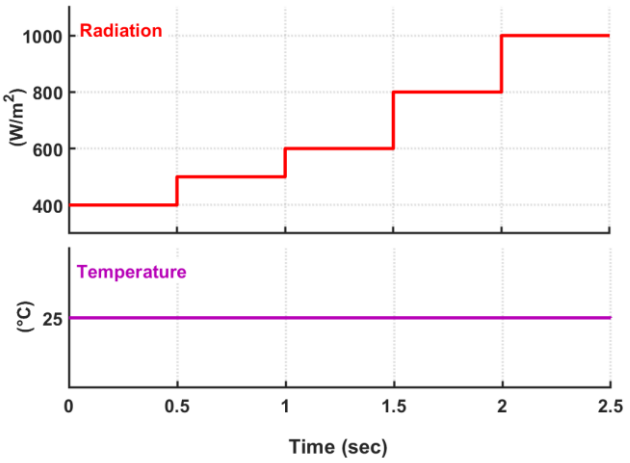

Fig. 19. Case 3: profile of solar irradiation and temperature.

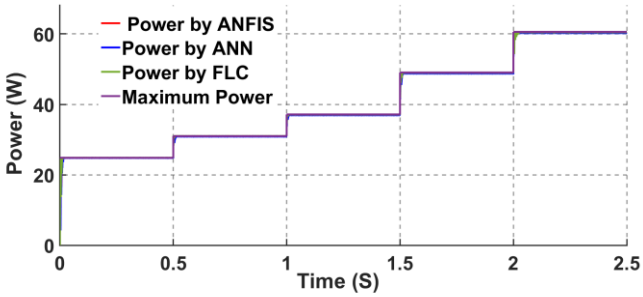

Fig. 20. Case 3: Performance of the ANFIS vs. ANN and FLC MPPT algorithms.

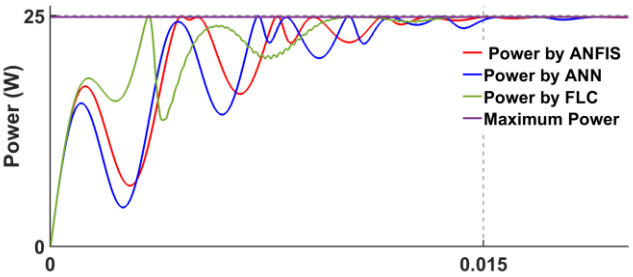

Fig. 21. Case 3: Dynamic response of ANFIS vs. ANN and FLC MPPT algorithms.

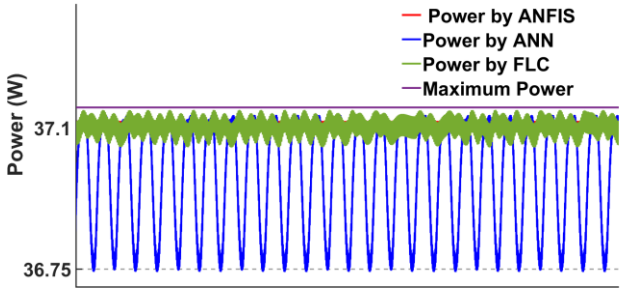

Fig. 22. Case 3: Steady-state power oscillation produced by ANFIS vs. ANN and FLC MPPT algorithms.

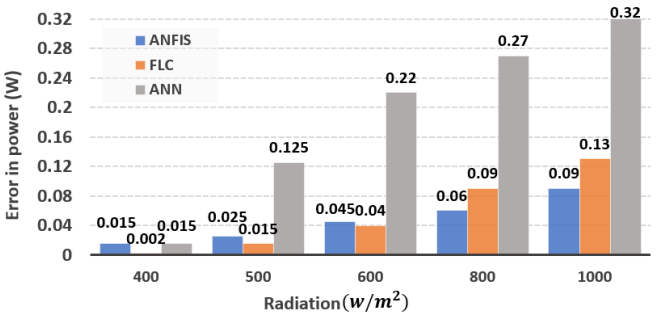

Fig. 23. Case 3: Error in Pmax at different radiation levels and constant temperatures using ANFIS, FLC, and ANN techniques.

Finally, in the last case (case 4): the temperature will gradually increase from 10 °C to 50 °C with step 5 °C. While the solar irradiation is changed between the levels of 400 W/m^2 and 1000 W/m^2 (i.e., 500 W/m^2, 600 W/m^2, 800 W/m^2). The PV system performance using the ANFIS, ANN, and FLC techniques is illustrated in Fig. 25. Fig. 26 reveals that the converging time of power tracking for the proposed ANFIS and FLC is 0.015 s, while the ANN captures MPP after 0.02 s with irradiation 400 W/m^2. With an irradiation level of 800 W/m^2 and a temperature of 40 °C, the uncertainties of the output power around the MPP were decreased to 0.05 % with the present controller, opposed to 0.4 % for the FLC and 0.74 % for the ANN algorithm, as given in Fig. 27.

Additionally, Fig. 28 exhibits the error in maximum power at varying levels of irradiation and temperature using the ANFIS, FLC, and ANN approaches. The ANFIS controller consistently records negligible percentage error in the maximum power output in all operational scenarios. This confirms that the introduced controller technique can capture the highest amount of power from the PV generators under different weather circumstances.

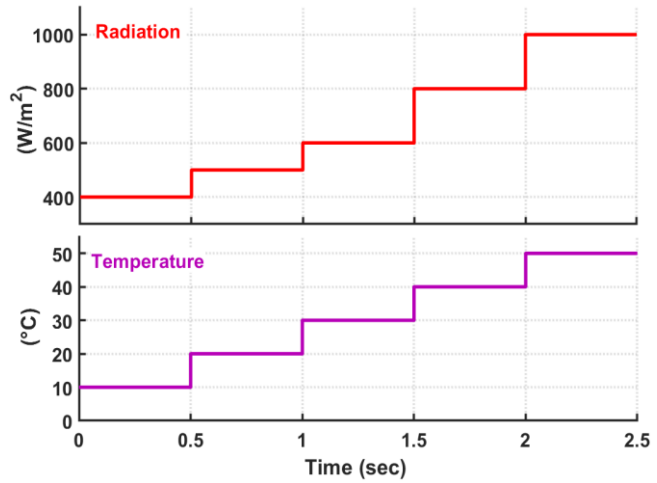

Fig. 24. Case 4: profile of solar irradiation and temperature.

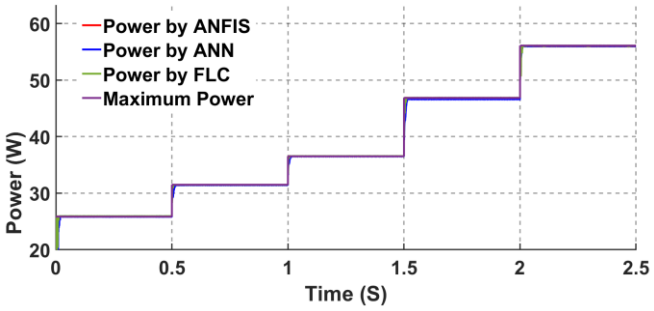

Fig. 25. Case 4: Performance of the ANFIS vs. ANN and FLC MPPT algorithms.

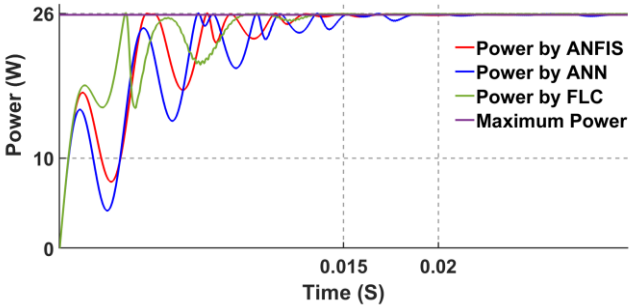

Fig. 26. Case 4: Dynamic response of ANFIS vs. ANN and FLC MPPT algorithms.

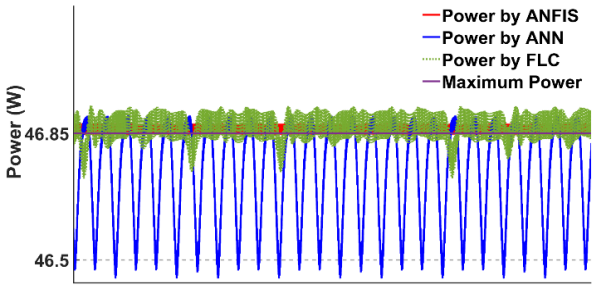

Fig. 27. Case 4: Steady-state power oscillation produced by ANFIS vs. ANN and FLC MPPT algorithms.

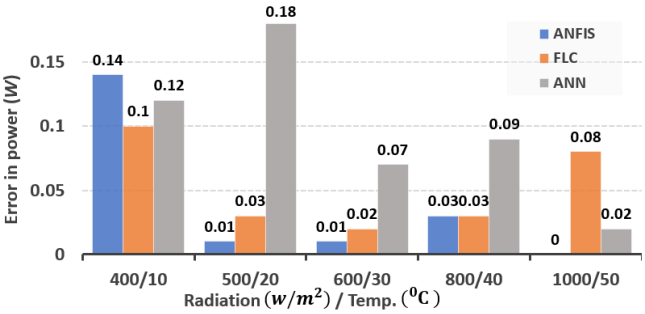

Fig. 28. Case 4: Error in Pmax at different radiation levels and temperatures using ANFIS, FLC, and ANN techniques.

6. Conclusion

This article proposes an efficient, reliable, simple, and robust ANFIS-MPPT technique for stand-alone PV generators. In this method, the MPPT control loop was simplified by eliminating the PI controller; hence, the computational and evaluation process for optimizing the gains of the PI controller was omitted. Further, the duty cycle

can be set instantly in the MPPT technique. The proposed ANFIS model is based on reliable training data generated using the MV-PO MPPT algorithm. It is precise, easy to use, and requires little experimental training data. The obtained results exhibit that the proposed controller tracked the maximum available amount of electrical power for the overall range of radiation with more real profiles. In other words, The ANFIS-MPPT method is more rapid than the FLC and ANN algorithms. As a result, the proposed ANFIS-MPPT controller furnishes a robust operation with a few oscillations that are not obvious.

Acknowledgments

The authors [Mohamed H. Osman and Mamdouh K. Ahmed] are funded by a scholarship [Ph.D.] under the joint (executive program between the Arab Republic of Egypt and the Russian Federation).

References

[1] A. Belkaid, I. Colak, K. Kayisli, and R. Bayindir, "Improving PV System Performance using High Efficiency Fuzzy Logic Control", In 2020 8th International Conference on Smart Grid (icSmartGrid), pp. 152-156, IEEE, 2020.

[2] H. Alrajoubi, S. Oncu and S. Kivrak, "An MPPT Controlled BLDC Motor Driven Water Pumping System", 2021 10th International Conference on Renewable Energy Research and Application (ICRERA), pp. 116-119, 2021.

[3] A. I. Nusaif, and A. L. Mahmood, "MPPT Algorithms (PSO, FA, and MFA) for PV System Under Partial Shading Condition, Case Study: BTS in Algazalia, Baghdad", International Journal of Smart Grid-ijSmartGrid 4(3), pp. 100-110, 2020.

[4] S. Marhraoui, A. Abbou, N. El Hichami, S. E. Rhaili and M. R. Tur, "Grid-Connected PV Using Sliding Mode Based on Incremental Conductance MPPT and VSC", 2019 8th International Conference on Renewable Energy Research and Applications (ICRERA), pp. 516-520, 2019.

[5] E. Mostafa, and N. K. Bahgaat, "A Comparison Between Using A Firefly Algorithm and A Modified PSO Technique for Stability Analysis of a PV System Connected to Grid", International Journal of Smart Grid-ijSmartGrid 1(1), pp. 1-8, 2017.

[6] A. Refaat, M. H. Osman, and N. V. Korovkin, "Current collector optimizer topology to extract maximum power from non-uniform aged PV array" Energy, 195, 116995.2020.

[7] S. Necaibia, M. S. Kelaiaia, H. Labar, A. Necaibia, and E. D. Castronuovo, "Enhanced auto-scaling incremental conductance MPPT method, implemented on low-cost microcontroller and SEPIC converter", Solar Energy, vol. 180, pp. 152–168, Mar. 2019.

[8] M. H. Osman, M. K. Ahmed, A. Refaat, and N. V. Korovkin, "A Comparative Study of MPPT for PV System Based on Modified Perturbation & Observation Method", In 2021 IEEE Conference of Russian Young Researchers in Electrical and Electronic Engineering (ElConRus), pp. 1023-1026, IEEE, 2021.

[9] U. Yilmaz, A. Kircay, and S. Borekci, "PV system fuzzy logic MPPT method and PI control as a charge controller", Renewable and Sustainable Energy Reviews, vol. 81, pp. 994–1001, Jan. 2018.

[10] B. Babes, A. Boutaghane, and N. Hamouda, "A novel nature-inspired maximum power point tracking (MPPT) controller based on ACO-ANN algorithm for photovoltaic (PV) system fed arc welding machines", Neural Computing and Applications 2021, pp. 1–19, Aug. 2021.

[11] M. H. Osman., M. A. Elseify, M. K. Ahmed, N. V. Korovkin, & A. Refaat, "Maximum Power Point Tracking for Grid-tied PV System Using Adaptive Neuro-Fuzzy Inference System", In 2021 International Conference on Electrotechnical Complexes and Systems (ICOECS), pp. 534-540, IEEE, 2021.

[12] M. Abdel-Salam, M. T. El-Mohandes, and M. Goda, "An improved perturb-and-observe based MPPT method for PV systems under varying irradiation levels", Solar Energy, vol. 171, pp. 547–561, Sep. 2018.

[13] B. R. Peng, K. C. Ho, and Y. H. Liu, "A Novel and Fast MPPT Method Suitable for Both Fast Changing and Partially Shaded Conditions", IEEE Transactions on Industrial Electronics, vol. 65, no. 4, pp. 3240–3251, Apr. 2018.

[14] M. Pokharel, A. Ghosh, and C. N. M. Ho, "Small-Signal Modelling and Design Validation of PV-Controllers with INC-MPPT Using CHIL", IEEE Transactions on Energy Conversion, vol. 34, no. 1, pp. 361–371, Mar. 2019.

[15] N. Kumar, B. Singh, B. K. Panigrahi, and L. Xu, "Leaky-Least-Logarithmic-Absolute-Difference-Based Control Algorithm and Learning-Based InC MPPT Technique for Grid-Integrated PV System", IEEE Transactions on Industrial Electronics, vol. 66, no. 11, pp. 9003–9012, Nov. 2019.

[16] M. A. Danandeh and S. M. Mousavi G., "Comparative and comprehensive review of maximum power point tracking methods for PV cells", Renewable and Sustainable Energy Reviews, vol. 82, pp. 2743–2767, Feb. 2018.

[17] N. Kumar, B. Singh, B. K. Panigrahi, C. Chakraborty, H. M. Suryawanshi, and V. Verma, "Integration of solar PV with low-voltage weak grid system: Using normalized laplacian kernel adaptive kalman filter and learning based InC algorithm", IEEE Transactions on Power Electronics, vol. 34, no. 11, pp. 10746–10758, Nov. 2019.

[18] L. L. Jiang, D. R. Nayanasiri, D. L. Maskell, and D. M. Vilathgamuwa, "A hybrid maximum power point

tracking for partially shaded photovoltaic systems in the tropics", Renewable Energy, vol. 76, pp. 53–65, Apr. 2015.

[19] Y. Wang, Y. Yang, G. Fang, B. Zhang, H. Wen, H. Tang, L. Fu, and X. Chen, "An Advanced Maximum Power Point Tracking Method for Photovoltaic Systems by Using Variable Universe Fuzzy Logic", Control Considering Temperature Variability," Electronics 2018, Vol. 7, Page 355, vol. 7, no. 12, p. 355, Nov. 2018.

[20] X. Li, H. Wen, Y. Hu, and L. Jiang, "A novel beta parameter based fuzzy-logic controller for photovoltaic MPPT application", Renewable Energy, vol. 130, pp. 416–427, Jan. 2019.

[21] M. Lasheen and M. Abdel-Salam, "Maximum power point tracking using Hill Climbing and ANFIS techniques for PV applications: A review and a novel hybrid approach", Energy Conversion and Management, vol. 171, pp. 1002–1019, Sep. 2018.

[22] M. S. F. Bangi and J. S. il Kwon, "Deep hybrid modeling of chemical process: Application to hydraulic fracturing",Computers & Chemical Engineering, vol. 134, p. 106696, Mar. 2020.

[23] R. K. Kharb, S. L. Shimi, S. Chatterji, and M. F. Ansari, "Modeling of solar PV module and maximum power point tracking using ANFIS", Renewable and Sustainable Energy Reviews, vol. 33, pp. 602–612, May 2014.

[24] A. M. S. Aldobhani, R. John, "Maximum power point tracking of PV system using ANFIS prediction and fuzzy logic tracking", Int. Multi Conference Eng. Comput. Sci. (IMECS). 2, pp. 19–21, 2008.

[25] S. D. Al-Majidi, M. F. Abbod, & H. S. Al-Raweshidy. "Design of an efficient maximum power point tracker based on ANFIS using an experimental photovoltaic system data", Electronics 8(8), 858, 2019.

[26] M. Lasheen, and A. Mazen, "Maximum power point tracking using Hill Climbing and ANFIS techniques for PV applications: A review and a novel hybrid approach", Energy conversion and management, 171, pp. 1002-1019, 2018.

[27] H. Afghoul; F. Krim, and D. Chikouche, "Increase the photovoltaicconversion efficiency using neuro-fuzzy control applied to MPPT", Renew. Sustain. Energy Conf. (IRSEC), pp.,348–353, 2013.

[28] A. Iqbal, H. Abu-Rub; S. M. Ahmed, "Adaptive neuro-fuzzy inference system based maximum power point tracking of a solar PV module", IEEE International Energy Conference and Exhibition (EnergyCon), pp. 51–56, 2010

[29] R. K. Kharb, S. L. Shimi, S. Chatterji, and M. F. Ansari, " Modeling of solar PV module and maximum power pointtracking using ANFIS", Renew. Sustain. Energy Rev. 33, pp. 602–612, 2014.

[30] T. Weldcherkos, A. O. Salau, and A. Ashagrie, "Modeling and design of an automatic generation control for hydropower plants using Neuro-Fuzzy controller", Energy Reports, vol. 7, pp. 6626–6637, Nov. 2021.

[31] M. H. Osman and A. Refaat, "Adaptive multi-variable step size P&O MPPT for high tracking-speed and accuracy," in IOP Conference Series: Materials Science and Engineering, vol. 643, no. 1. Nov. 2019.

[32] M. I. El-Sayed, M. A. E. H. Mohamed, and M. H. Osman, "A novel parameter estimation of a PV model", In 2016 IEEE 43rd Photovoltaic Specialists Conference (PVSC) pp. 3027-3032, IEEE, 2016.